

Parametrization of mesoscale and small-scale orography effects in HIRLAM - final tests

Laura Rontu (FMI) Kai Sattler (DMI) Mariken Homleid (met.no)

1 Introduction

In the present reference HIRLAM, all subgrid-scale orography effects are parametrized using the concept of effective orographic roughness (Undén et al., 2002). Calculation of this parameter has been recently improved (Sattler, 2004a,b) and its application for calculation of surface layer turbulent momentum fluxes updated. Because of practical and theoretical problems of the effective roughness method, an alternative, scale-dependent approach for parametrization of orographic momentum fluxes has been developed and validated during several years, see Rontu et al. (2002); Rontu (2006) also several Newsletter contributions (Sigg, Rontu, Sattler in NL37, NL38, NL41, NL44, NL45). It consists of a parametrization of the effects of mesoscale orography (MSO): buoyancy waves and blocking of stable air by mountains, developed for Meteo France ARPEGE system (Geleyn et al., 1994); and those of small-scale orography (SSO): turbulent momentum fluxes due to kilometre-scale orography, based on ideas by Wood et al. (2001).

In this report, we summarise the latest updates to the MSO/SSO parametrizations, document the method of derivation of the needed orography parameters within the HIRLAM climate generation system and report results of verification against ten-metre winds observed at Norwegian synoptic stations in January 2005.

2 Updated MSO/SSO parametrizations

The formulation of MSO parametrizations adapted for HIRLAM remains as documented in Rontu et al. (2002). Meanwhile, the original Meteo France MSO scheme has undergone significant modifications recently documented and validated by Geleyn et al. and Catry et al. (unpublished manuscripts, 2006). Possible implementation of these new features is left for further studies in the common IFS framework of HIRLAM-ALADIN physics.

Three small changes were made to the SSO parametrizations compared to Rontu (2006). First, the parametrized surface orographic stress $\vec{\tau}_{os} = C_o \frac{\vec{\tau}_{ts}}{\rho_s} s_t^2$ (where C_o is SSO drag coefficient, $\vec{\tau}_{ts}$ denotes surface turbulent stress, ρ_s is surface air density and s_t is the SSO slope parameter) is added to the surface turbulent stress and transmitted to the vertical diffusion (CBR) scheme, instead of using a simple exponential decay of the stress suggested by Wood et al. (2001) and used by Rontu (2006). Thus the SSO standard deviation is presently not needed by the scheme, but the only SSO-related parameter is s_t . Second, this SSO slope s_t is calculated as a part of HIRLAM climate generation system as described in Sec. 3 below, instead of using the external to HIRLAM

methods of the earlier tests (Rontu, 2003, 2006).¹ Third, the value of the coefficient C_o was changed and made dependent on the lowest model level wind velocity. Now $C_o = C_{oo}V_o/(V_{nlev} + V_o)$, where V_{nlev} denotes the lowest model level wind speed, $C_{oo} = 100$ and $V_o = 1$ m/s. The idea was to increase the drag on the weakest winds.

3 Preparation of the orography parameter fields

Both the MSO and the SSO parametrization schemes need information about the underlying orography beyond the resolved grid scale of the model. The sub-grid orography properties are represented by a number of parameters supposed to describe the impact of orography from the smallest scales, where the SSO scheme applies, and from the meso-scales, where the MSO scheme is employed. Table 1 lists these parameters.

Table 1: Orography parameters for the MSO/SSO parametrization

parameter	description	unit	usage	orography filter
s_t	mean maximum small scale slope	rad	SSO	high-pass
σ_t	mean small scale standard deviation	J/kg	SSO	high-pass
σ_m	mean meso scale standard deviation	J/kg	MSO	band-pass
α	coefficient of anisotropy	-	MSO	band-pass
Θ	x-angle of orography gradient	rad	MSO	band-pass

The derivation of the orography parameters for SSO and MSO is based on differently filtered orography data (see Table 1). Determination of the SSO parameters is described by Rontu (2003). This methodology has been adopted for the Hirlam climate generation (physiographic and surface data preprocessing). Concerning the MSO parameters, these are described in Rontu et al. (2002) and Undén et al. (2002). They are based on a band-pass filtered orography. The aggregation of the MSO/SSO parameters is to be included into the climate generation of Hirlam by version 7.1. The following two sections describe more details of the implementation.

3.1 SSO parameter aggregation

The aggregation of s_t consists of a simple averaging of the field of maximum slope provided by the HDF files data base. This field has been determined on basis of Eq. (8) of Rontu (2003).

Aggregation of σ_t is done using the non-linear aggregation methodology for aggregation of subgrid-scale orography roughness (Sattler, 2004b). The ingoing height field is, however, based on the filtered height h' of Eq. (8) of Rontu (2003). The formulation for σ_t then reads

$$\sigma_t^2 = \frac{1}{\sum_{j=1}^J K_j} \sum_{j=1}^J \sum_{k=1}^{K_j} h_{j,k}'^2 - \left(\frac{1}{\sum_{j=1}^J K_j} \sum_{j=1}^J \sum_{k=1}^{K_j} h_{j,k}' \right)^2, \quad (1)$$

with K_j denoting the number of original grid pixels within a source grid pixel (original data field). The sums over k are provided through the HDF files, and the summation over j is done during

¹Note that the SSO slope values shown in Table 1 and Fig. 3 of (Rontu, 2006) contain a conversion error: they should be multiplied by a coefficient 5.7, i.e. $s_t(\text{correct})=5.7 s_t(\text{article})$

climate generation. K_j is also provided through the HDF files. σ_t is scaled with the gravity constant of the earth to represent units of J/kg.

3.2 MSO parameter aggregation

The parameters for the MSO parametrization scheme comprise the isotropic parameter σ_m and the two anisotropic parameters α and Θ . σ_m is aggregated during climate generation and scaled to units of J/kg using the Earth's gravity constant. α and Θ are based on the tensor of orographic gradient correlation (Rontu et al., 2002), which is aggregated during climate generation using the methodology of *subdivided aggregation grid* described in section 2.2.2 of Sattler (2001). α and Θ are then determined from this aggregated field in a separate routine during climate generation.

All the aggregations described in the previous paragraph are based on a band-pass filtered orography. The band-pass filter has been described in Rontu et al. (2002) and reads:

$$h_{\text{bpf}}(x) = h_L \left(1 - \frac{\int_{-\infty}^{\infty} g(x-x') h_L(x') dx'}{\int_{-\infty}^{\infty} g(x-x') dx'} \right), \quad (2)$$

with

$$g(x-x') = \exp \left(-\frac{2|x-x'|}{\delta} \right)^a. \quad (3)$$

h_L denotes the low-pass filtered orography, and δ is the scale parameter determining the limits for taking large scales into account (`MSO_BPF_LOW` in the `Climate` script).

The value of a has been set to 2 here.

The band-pass filter is going to be implemented in an approximated form into the Hirlam reference system from version 7.1 on. The implementation consists of two steps. Firstly, h_L is realized through the HDF files with a fixed small scale limit (`MSO_BPF_HIGH` in the `Climate` script) of 0.025° .² Secondly, the aggregation of h_{bpf} is done during the climate generation on basis of h_L from the HDF files.

Applied on the discrete gridded orography fields from the HDF files, the integrals of (2) are represented by summation, and the limits do not go beyond the area of the domain. Summation to these limits, however, would demand an enormous computational effort, still. In order to limit the computational resources needed for the aggregation, the summation has been limited as follows:

$$h_{\text{abpf}}(x) = h_L \left(1 - \frac{\sum_{-\frac{3}{2}\delta}^{\frac{3}{2}\delta} g(x-x') h_L(x') dx'}{\sum_{-\frac{3}{2}\delta}^{\frac{3}{2}\delta} g(x-x') dx'} \right). \quad (4)$$

This is a restriction of the limits to a small multiple of the scale parameter δ . Beyond this limit, the contribution of the heights are very small and they are therefore neglected (Fig. 1).

In order to get a rough picture about the band-pass filter properties in practice, power spectral density estimations (PSDE, 2D-periodograms) have been applied on the orography fields and are shown in Fig. 2. "HDF 9000" (black) represents the PSDE of the orography from the Central European tile of the HDF file from the 9000 HDF set. This tile represents a central part of the input orography, and the PSDE follows closely the $k^{-5/3}$ dependence of the mesoscale atmospheric kinetic energy spectrum (see e.g. Skamarock (2004) and references herein). The k^{-3}

²This necessitates use of the `HDFSET 9000` or `regular` with `HIRES=0.025` or `0.0125`.

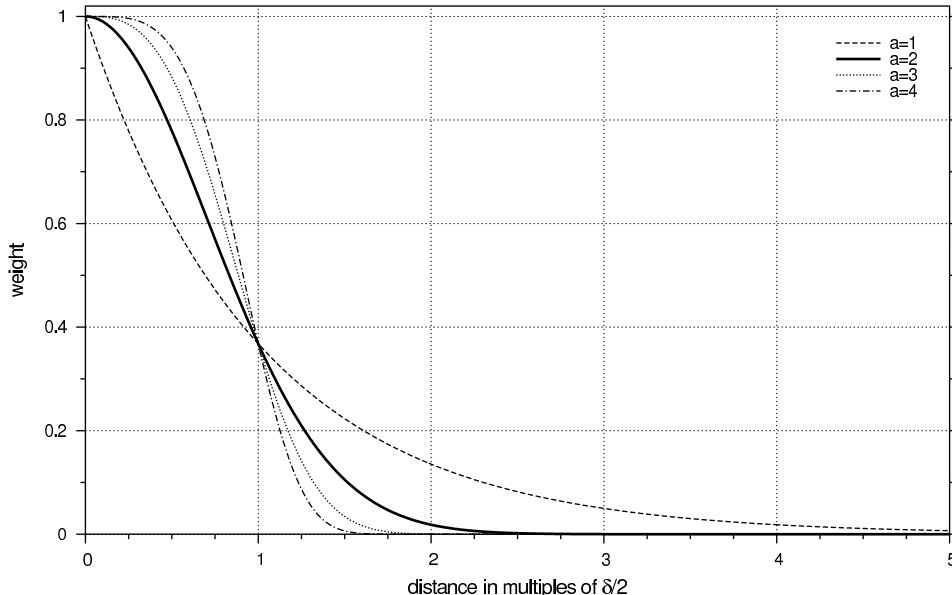


Figure 1: *Weighting factors for height pixels as a function of the distance from the centre pixel, for different values of a (Eq. (3)). For the MSO band-pass filter $a=2$, and weights beyond distances of $3\frac{\delta}{2}$ are very small and therefore neglected.*

relation for large scale atmospheric spectra is also shown in Fig. 2 for comparison. The resolution of the grid (0.025 degrees) ends at a wavenumber slightly larger than 0.001m^{-1} , corresponding to the $2\text{-}\Delta x$ scale of the grid mesh. Towards the large scales on the left-hand side of the plot the curves may become imprecise due to the limited domain size.

"raw" in Fig. 2 (red) denotes the spectrum from the normal height field aggregated for the RCR domain. It is filtered for Hirlam using an implicit filter of Raymond (1988), which is shown by the curve "filtered" (green). This is the spectrum from the orography as the Hirlam model "sees" it. The filtering is to reduce the smallest grid scales close to the resolution limit of the RCR grid at wavenumbers around 0.00014m^{-1} . The unsteadiness in the PSDE curves close to the high resolution limit of the grid is due to the fact that the grid mesh sizes are specified in degrees of rotated geographic coordinates, which results in differences in the geometric mesh size (given in km) in x- and in y-direction.

As mentioned above, the MSO parameter aggregation is done in two steps. The first step is the aggregation of the low-pass filtered orography h_L , which in this case just consists of a normal aggregation of height for the area of the RCR domain on basis of the HDF files, but with a grid of mesh size equal to the HDF file, i.e. 0.025° . This low-pass filtered orography is shown in Fig. 2 as "LPF RCR" in light blue. The spectrum of this orography coincides well with the "HDF 9000" in the large scale range. Minor differences occur due to different area size. At the small scale spectrum, however, "LPF RCR" has significantly lost power due to effects occurring during aggregation. Besides the difference in area size, the grid of "HDF 9000" and "LPF RCR" differ also in the grid rotation: The RCR domain is rotated with South Pole position 0° longitude and -30° latitude, whereas the HDF 9000 file is rotated with South Pole position 90° longitude and 0° latitude. This difference in rotation leads to aggregation effects like interpolation or small coordinate shifts during climate generation processing, which is believed to be responsible for the loss in small scale power.

The second step in the band-pass filter aggregation consists of the removal of the large scales

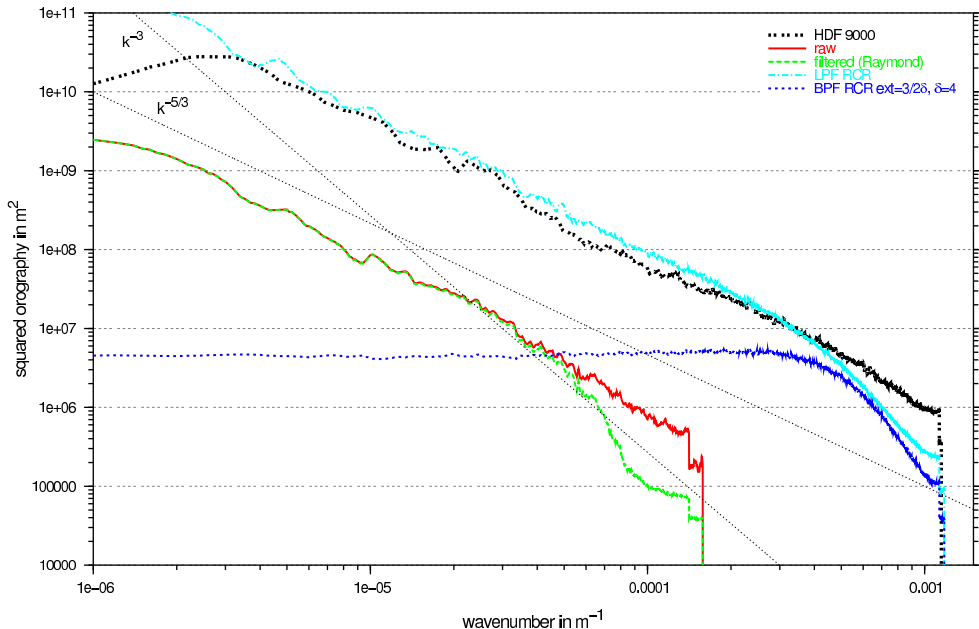


Figure 2: *Unsmoothed absolute power spectral density estimations (PSDE) of the height fields processed in the Hirlam climate generation for the RCR domain. See text for a detailed description of the curves. The black dotted sloping lines represent slopes of k^{-3} and $k^{-\frac{5}{3}}$.*

that are supposed to be resolved by the model. The dark blue curve in Fig. 2, "BPF RCR ext=3/2 δ , $\delta=4$ ", shows the PSDE of the filtered orography after this second step. The large scale filter limit is set to $\delta=4$ model grid units, and the extension of the sum in (4) is 3/2 δ .

This is the orography as it is used for the MSO parameter aggregations. The curve shows clearly effects from the filtering and some of the small scale power is further reduced, again presumably due to aggregation effects. Most power is found in the sub-grid range of the RCR grid, i.e. between wavenumbers around 0.001 and 0.00014 m^{-1} .

The reduction in power in the large scale range of "BPF RCR ext=3/2 δ , $\delta=4$ " (Fig. 2) is quite significant, and a part of this could be due to the filter approximation described by (4). For a rough comparison, the magenta curve in Fig. 3 ("BPF 9000 (2002)") shows the filtered orography as it was used in the work of Rontu et al. (2002), who used a different implementation of the band-pass filter. This orography was filtered outside the climate generation routines first, without approximation and on exactly the same grid as the orography from the HDF file. This orography may be regarded as a kind of ideally filtered orography³. This field was then aggregated on to the grid of the RCR domain, and the resulting field is shown by the grey curve in Fig. 3 ("BPF RCR (2002)"). Exactly as before the aggregation on to the RCR domain results in reduction of power at the smallest scales. The dark blue curve of "BPF RCR ext=3/2 δ , $\delta=4$ " is also plotted into Fig. 3 for comparison.

Most of the remaining differences of the PSDE of "BPF RCR ext=3/2 δ , $\delta=4$ " and "BPF RCR (2002)" occur in the large scale range of the spectrum. They seem, however, not just directly related to the approximation described in (4), because extending the sum in (4) to e.g. 6/2 δ does not change the PSDE ("BPF RCR ext=6/2 δ , $\delta=4$ " (yellow) in Fig. 3, lies virtually below the dark

³The reason why this approach has not been implemented into the reference system is that this approach necessitates a specific and tedious treatment at the tile borders of the HDF file data with some unresolved boundary effects.

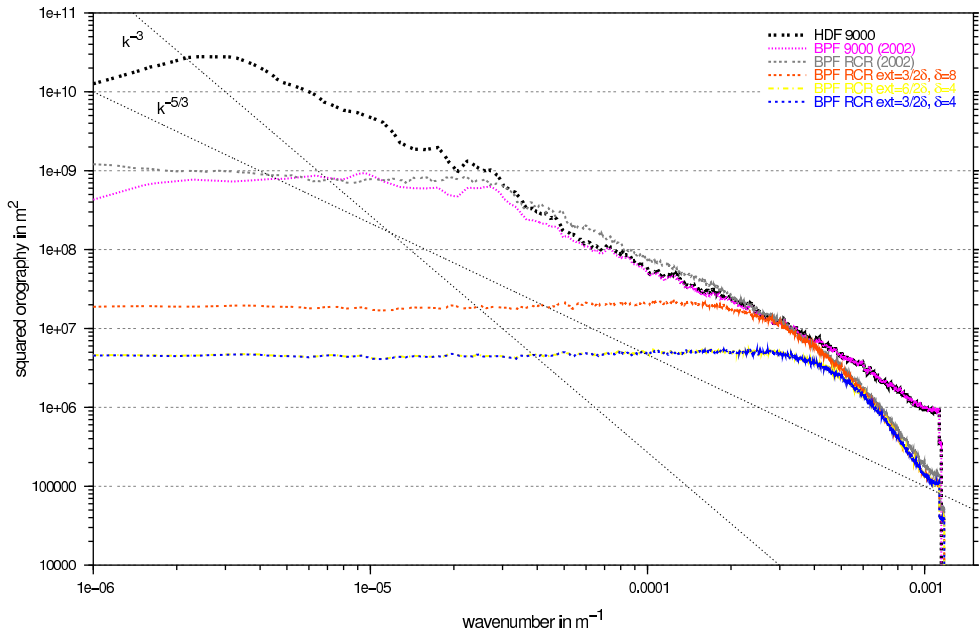


Figure 3: *Unsmoothed absolute power spectral density estimations (PSDE) of height fields related to the band-pass filter process. See text for a detailed description of the curves. The black dotted sloping lines represent slopes of k^{-3} and $k^{-\frac{5}{3}}$.*

blue curve). On the other hand, increase of the large scale filter limit δ (MSO_BPF_LOW) extends the spectrum towards larger scales, as expected ("BPF RCR ext=3/2 δ , $\delta=8$ " (orange) in Fig. 3).

4 January 2005 validation

4.1 Description of the experiments

The suggested parametrizations were tested in one-month (11 km resolution) and two-week (4 km resolution) model experiments over Scandinavian mountains. In addition to the standard verification, the ten-metre wind values were compared with the Norwegian observations. January 2005 was characterized with high cyclonic activity from Atlantic towards Scandinavia. Several storms occurred in the area during the period. Fig. 4 shows the experiment domains, with isolines of mean-sea-level pressure based on NOF (see Table 2 for the experiment definition) analyses averaged over 1 - 15 January. Table 2 shows the experimental setup. In all experiments, the number of levels in vertical was 40. Three-dimensional variational data-assimilation was applied in a cycle of 6 hours. Long forecasts till +48 (NOR and NOR) or +24h (SM4) were run starting at 00UTC and 12UTC only.

Table 2: January 2005 experiments

Experiment	HIRLAM version	resolution	schemes	boundaries
NOR	6.4.3	11 km	$z_{o,oro}$	RCR analyses
NOF	6.4.3	11 km	MSO/SSO	RCR analyses
SM4	6.4.3	4 km	MSO/SSO	NOF analyses

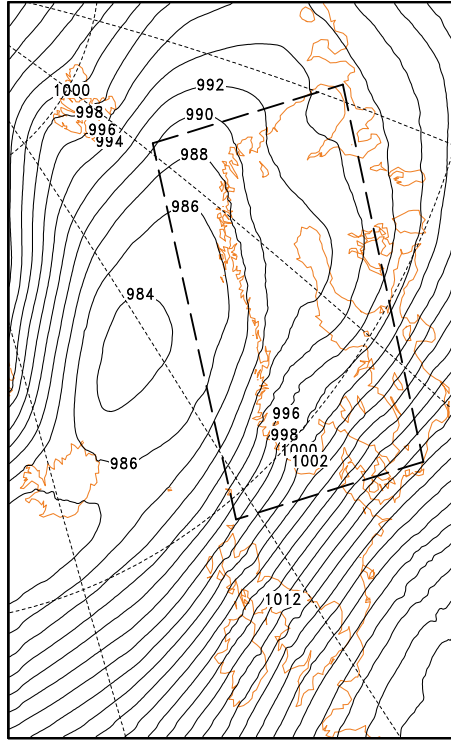


Figure 4: *Experiment domains: 11 km resolution (full map area) and 4 km (dashed-line box), with mean-sea level pressure from NOF analyses averaged over four daily analyses during 1-15 January.*

4.2 Standard verification of wind and pressure forecasts

In the standard station verification pictures (not shown) over Scandinavian or EWGLAM stations there is practically no difference between NOR and NOF forecasts in January 2005. Both show a positive mean sea level pressure bias of about one hPa and ten-metre wind bias of about one m/s. Fig. 5 shows the mean sea level pressure and ten-metre wind systematic error (fc-obs) of +24 hour forecasts of the experiments NOR, NOF and SM4 at all Norwegian WMO stations (block 1)⁴ used in HIRLAM analysis. All forecasts show a positive pressure bias, especially in the cases of low pressure. However, NOF and SM4 behave slightly better than the reference NOR. The positive bias of weak (wind speed less than ca. 8 m/s) winds increases in NOF compared to NOR but is about the same in NOR and the fine-resolution SM4. The strongest winds (wind speed more than ca. 15 m/s) are underpredicted by all experiments. Based on this comparison, no clear overall improvement or deterioration due to the new parametrizations is seen.

4.3 Results evaluated at Norwegian synoptic stations

At met.no, HIRLAM version 6.4.0 has been compared to the HIRLAM version 6.2.0 in 22 km resolution runs (not shown). It was found that v. 6.4.0 gave improved results for ten-metre wind as

⁴Note that the Arctic stations of Jan Mayen and Spitzbergen also belong to the WMO block 1. Their inclusion does not change the verification result essentially.

compared to v. 6.2.0. Most noticeable were the stronger winds in coastal zone. But in wind-exposed mountainous areas the wind speeds were still much too weak. Of the experiments of the present study, the features of the reference v. 6.4.3 experiment NOR come close to the earlier tested v. 6.4.0.

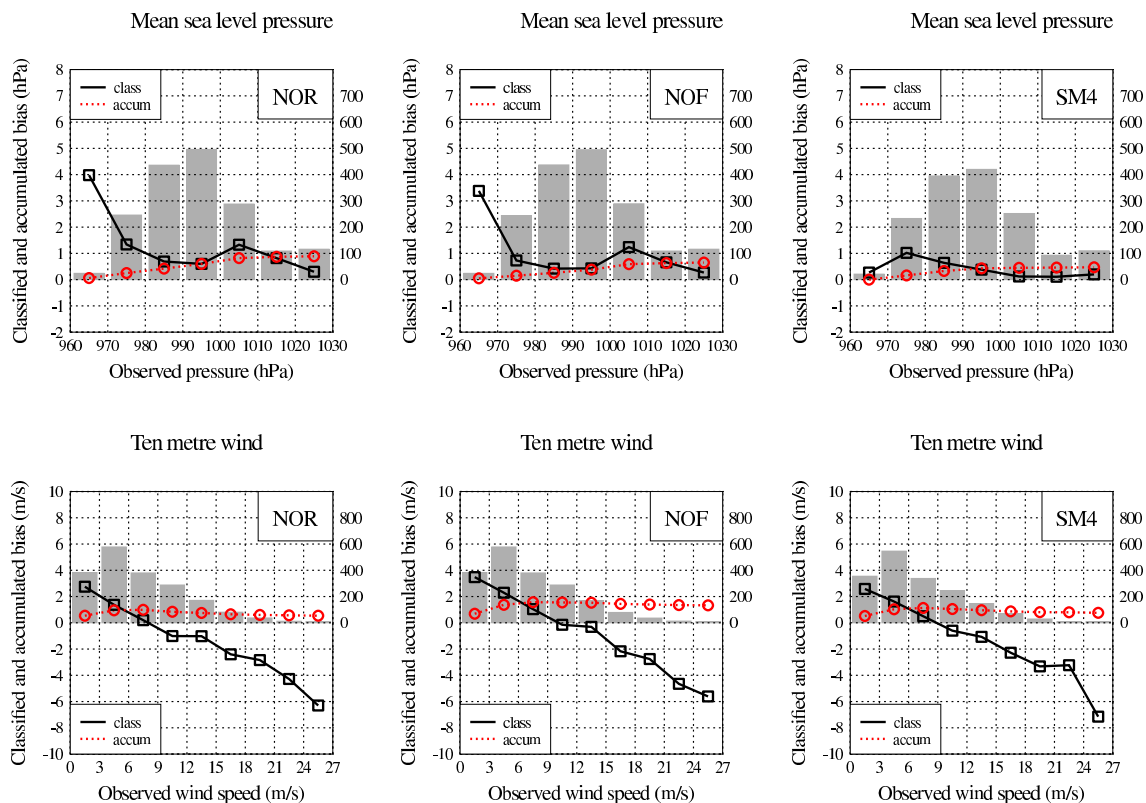


Figure 5: *Systematic difference between predicted and observed (00 UTC+24h forecasts - 00 UTC and 12 UTC observations) a) mean sea level pressure (hPa, upper panel, left y-axis) and ten-metre wind speed ($m s^{-1}$, lower panel, left y-axis) at the Norwegian synoptic stations in January 2005, 1-15, classified according to observed pressure (hPa, upper panel, x-axis) or wind ($m s^{-1}$, lower panel, x-axis). Number of observations in each class is shown by shaded bars (right y-axes). The lines with squares show the bias of each class. Lines with circles show the accumulated weighted contribution of the classes to the total bias of 00UTC+24h forecasts, which value is thus shown by the rightmost circle of each line. Experiments from left to right: NOR, NOF, SM4. Note that the amount of observations used in SM4 is smaller due to the smaller experiment domain.*

Experiments NOR, NOF and SM4 (see Table 2) were validated against 23 Norwegian synoptic stations during two first weeks of January 2005. Below the results from 7 to 15 January over chosen stations are shown. A map (Fig. 6) shows the location of the stations included into the present report. Ålesund-Vigra (WMO number 01210) is an airport which is sheltered from the strongest winds. It is quite close to Ona (01212), a station which is more wind-exposed. Finsevatn (01350), situated 1222 metres above the sea level, represents high-mountain environment while Gardemoen (02384) is located at flat area.

Three-hourly output of the experiments starting at 00 UTC is compared with SYNOP observations during the first +24 hours of the forecast: forecast 00 UTC + 3h v.s. SYNOP 03 UTC,

forecast 00 UTC + 6h v.s. SYNOP 06 UTC and so on. Thus the forecast length is different at different observation times. The results are shown in figs. 7 - 11. In addition to the coloured curves drawn, some self-explained statistical measures are included in the legend.

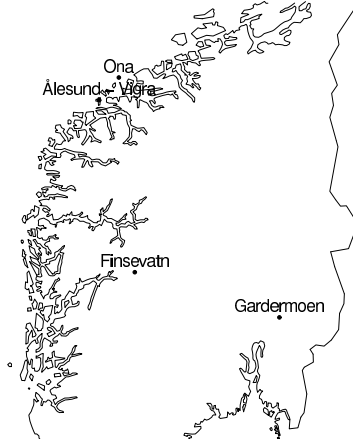


Figure 6: *Map of some Southern Norway stations.*

The NOF experiment with MSO/SSO parametrizations has significantly higher wind speeds over mountains, giving much better results there, as shown by Fig. 7 for Finsevatn. At the coastal stations the quality of NOR and NOF is similar, see Figs. 8 and 9. NOF has slightly more wind than NOR, that might give improved results at wind-exposed stations like Ona, but overestimation at stations in the fjords. At the flat land stations like Gardermoen (Fig. 10) the results for NOR and NOF are very close. The comparisons of 4 km and 10 km results (SM4 and NOF) show that SM4 generally has slightly less wind, and better results than NOF at many locations, see e.g. the time series from Ålesund-Vigra (Fig. 11).

5 Practical aspects of the implementation

Practical implementation of the new MSO and SSO schemes was done in the framework of HIRLAM physical parametrizations. The needed orography fields enter to forecast model from the physiography (climate) fields, going through several levels of code to the subroutines where they are actually used. The amount of calculations during the forecast run increased somewhat, leading to an estimated increase in the computing time of the order of eight per cent. In addition to the new input fields, new diagnostic output of small- and mesoscale surface stress components plus optional three-dimensional tendencies of wind components due to the momentum flux divergence is created. This leads to a small increase of required disk space and run-time memory. During climate generation, the band-pass filtering of the MSO parameters requires significantly more computing time, but is only necessary once for each experimental domain, as long as the filter properties are unchanged. For a smooth transition from the old to the new parametrizations, a switch between orographic roughness method and MSO/SSO parametrizations will be provided.

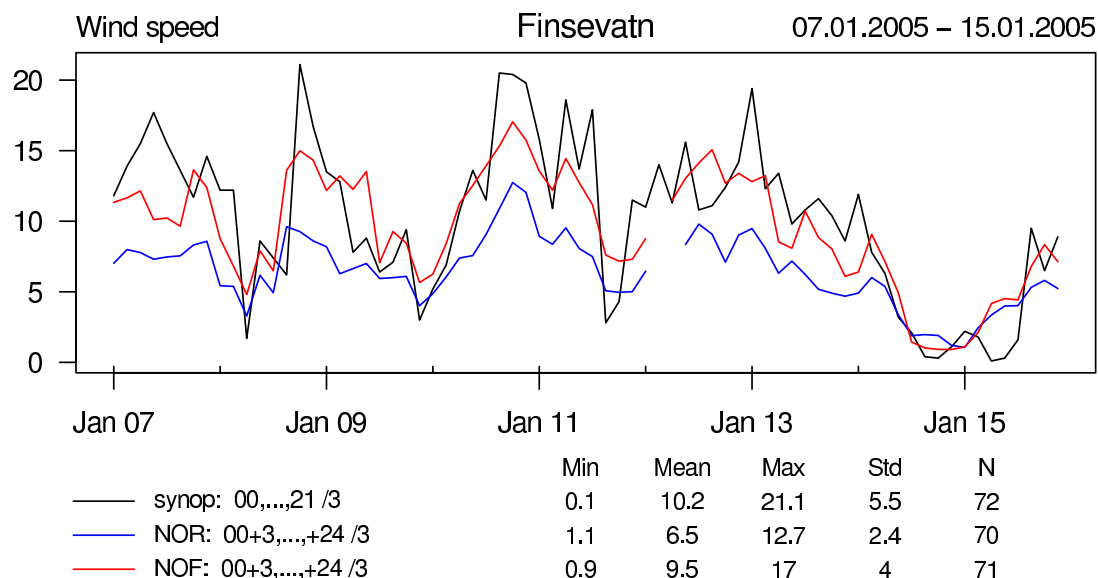


Figure 7: *Time series of NOR and NOF experiments compared with wind speed observed at mountain station Finsevatn (01350). See legend for details.*

6 Conclusions and further plans

New parametrizations of the mesoscale and small-scale orography effects were tested in the reference HIRLAM version 6.4.3. A method of calculation of the needed orography parameters is introduced into the reference HIRLAM v. 7.1 climate generation system. Validation against the Norwegian wind observations showed improved performance over the mountain stations compared to the present reference system. Overestimation of the dominating weaker winds and underestimation of the few cases of very strong wind remains a problem over flat areas and over the sea. The new parametrizations are ready for implementation to a next reference HIRLAM version.

Tuning and validation of the schemes will continue in comparative climate runs over North America, where the same MSO and SSO parametrizations (but including the updated Meteo France MSO scheme) are being introduced to the climate version of WRF by the researchers of University of Illinois. Also, case studies in some recent storm cases are planned in order to find possibilities to improve the ten-metre wind behaviour also by improvements in the turbulence scheme (vertical diffusion). Further development and application of the parametrizations in the meso-gamma-scale HIRLAM-AROME will raise new questions e.g. about the role of turbulence parametrizations in handling breaking of the mountain waves resolved by the fine-scale model. More practical tasks will be related to the climate generation in the IFS framework.

References

Geleyn, J.-F., E. Bazile, P. Bougeault, M. Déqué, V. Ivanovici, and coauthors, 1994: Atmospheric parametrisation schemes in Météo-France's ARPEGE N.W.P. model. Proc. Seminar on Physical Parametrization for Numerical Models. ECMWF, Shinfield Park, Reading, Berkshire, U.K., 385-402.

- Raymond, W. H., 1988: High-order low-pass implicit tangent filters for use in finite area calculations. *Mon. Wea. Rev.*, **116**, 2132–2141.
- Rontu, L., 2003: Derivation of orography-related climate variables for a fine resolution hirlam. *HIRLAM Newsletter*, (44), 83–96, Available at <http://hirlam.knmi.nl>.
- Rontu, L., 2006: A study on parametrization of orography-related momentum fluxes in a synoptic-scale NWP model. *Tellus*, **58A**, 69–81.
- Rontu, L., K. Sattler, and R. Sigg, 2002: Parametrization of subgrid-scale orography effects in HIRLAM. Technical Report 56, HIRLAM, 46pp. Available at <http://hirlam.knmi.nl>.
- Sattler, K., 2001: Aggregation of subgrid orography parameters in the hirlam climate system. *HIRLAM Newsletter*, (38), 122–126, Available at <http://hirlam.knmi.nl>.
- Sattler, K., 2004a: Non-linear aggregation of subgrid-scale orography roughness. *HIRLAM Newsletter*, (45), 124–140, Available at <http://hirlam.knmi.nl>.
- Sattler, K., 2004b: Corrigendum on non-linear aggregation of subgrid-scale orographic roughness. *HIRLAM Newsletter*, (46), 70–71, Available at <http://hirlam.knmi.nl>.
- Skamarock, W., 2004: Evaluation mesoscale NWP models using kinetic energy spectra. *Mon. Wea. Rev.*, **132**(12), 3019–3032.
- Undén, P., L. Rontu, H. Järvinen, P. Lynch, J. Calvo, and coauthors, 2002: The HIRLAM-5 Scientific documentation, December 2002. Available at <http://hirlam.knmi.nl>.
- Wood, N., A. R. Brown, and F. E. Hewer, 2001: Parametrizing the effects of orography on the boundary layer: An alternative to effective roughness lengths. *Quart. J. Roy. Met. Soc.*, **127**, 759–777.

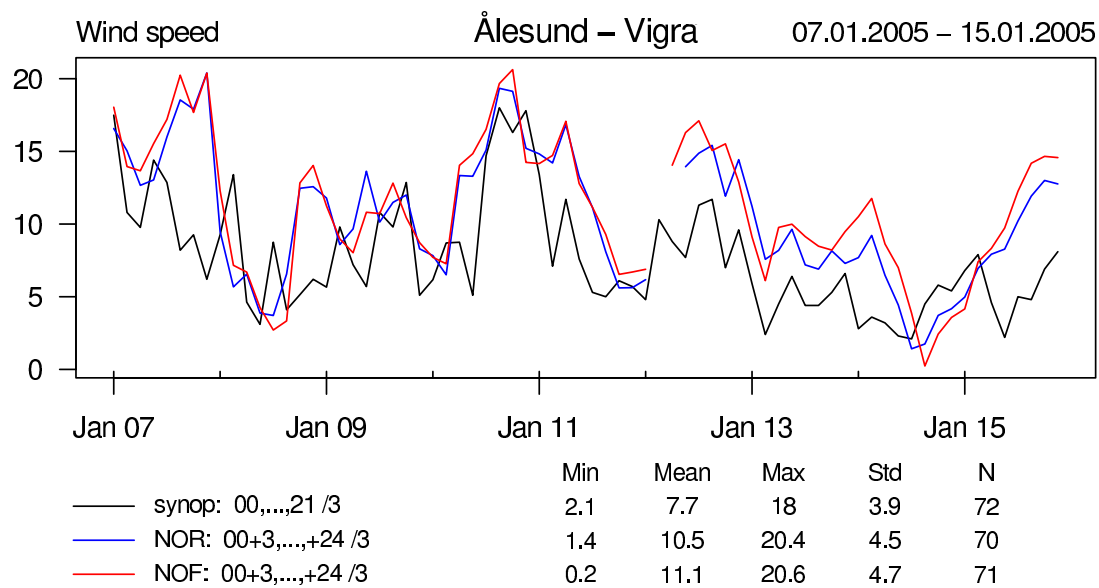


Figure 8: As Fig. 7 but for coastal station Ålesund-Vigra (01210).

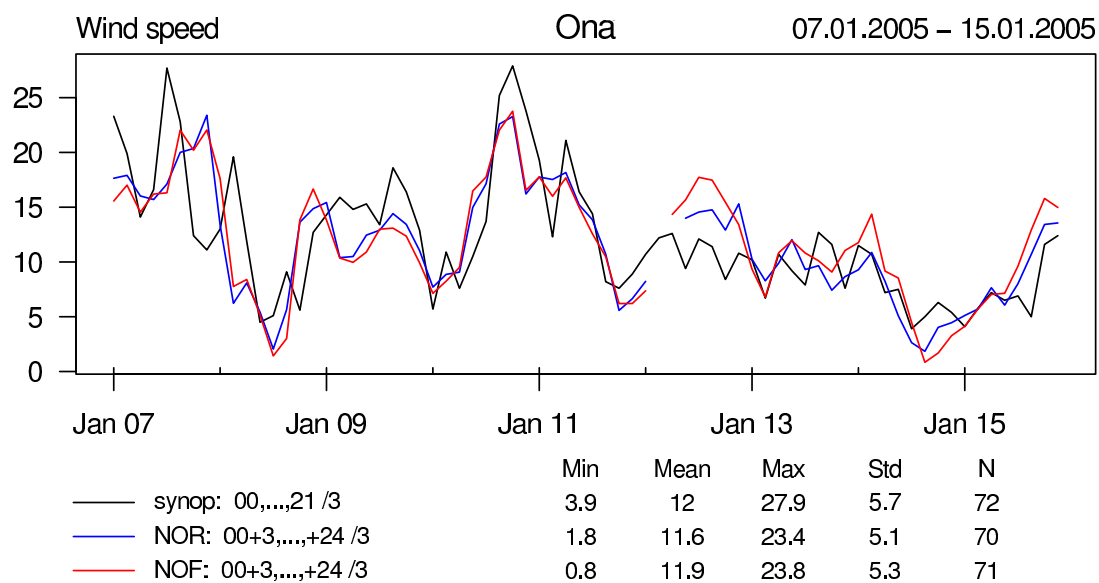


Figure 9: As Fig. 7 but for coastal station Ona (01212).

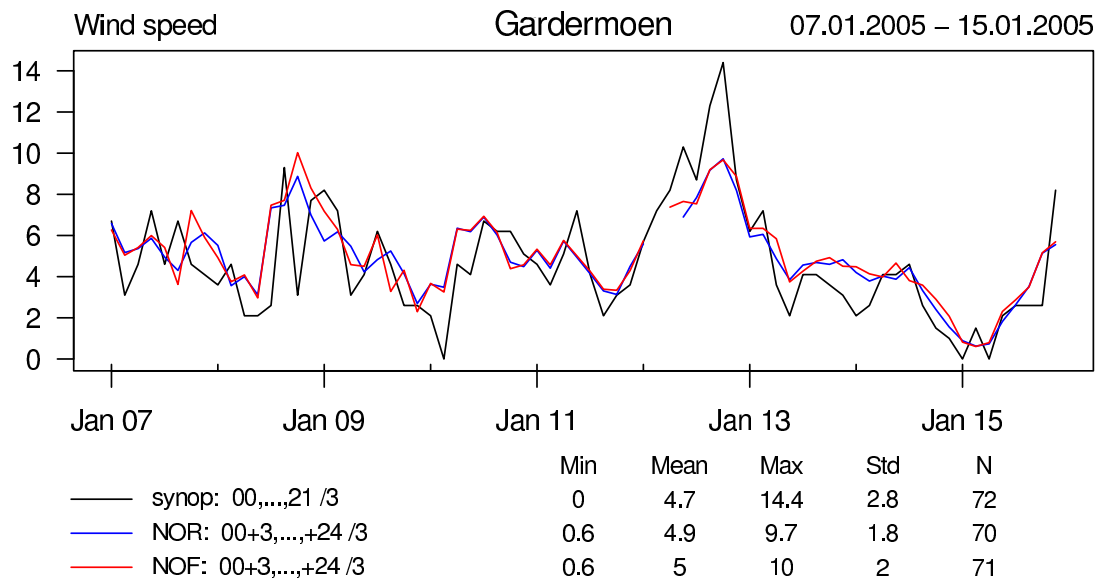


Figure 10: As Fig. 7 but for flat inland station Gardemoen (01384).

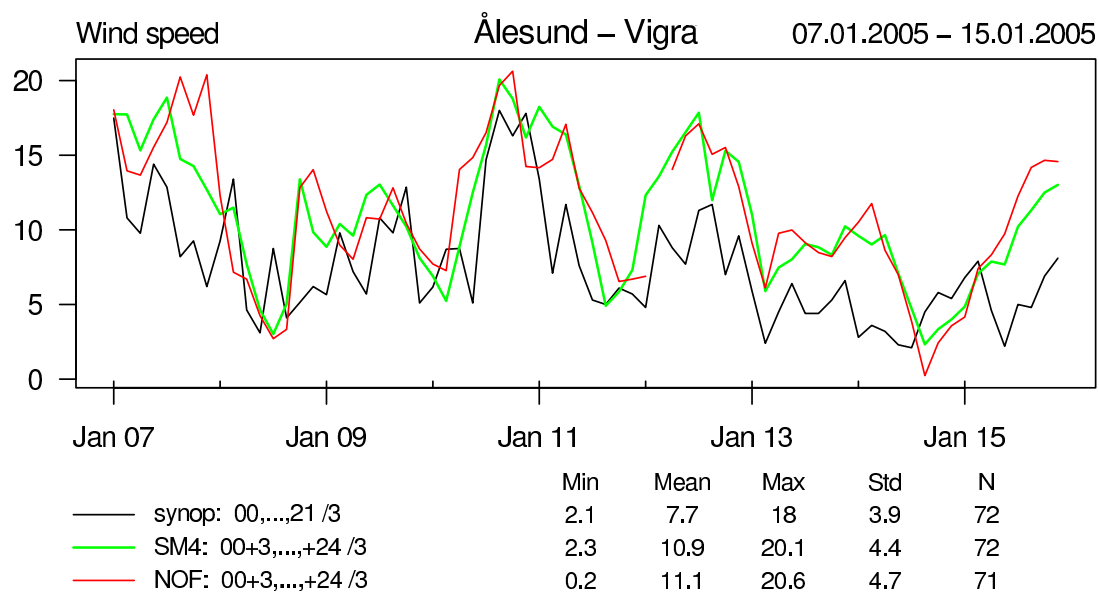


Figure 11: As Fig. 7 but for experiments SM4 and NOF at Ålesund-Vigra (01210).